Sensors and Actuators A 165 (2011) 26–34

Contents lists available at ScienceDirect

Sensors and Actuators A: Physical

journal homepage: www.elsevier.com/locate/sna

Micromachined rate gyroscope architecture with ultra-high quality factor and improved mode ordering

Alexander A. Trusov*, Adam R. Schofield, Andrei M. Shkel

MicroSystems Laboratory, Department of Mechanical and Aerospace Engineering University of California, Irvine, CA, USA

ARTICLE INFO

Article history:
Available online 18 January 2010

Keywords:
MEMS vibratory gyroscopes
Tuning fork
High-Q design

ABSTRACT

This paper reports a new dual mass vibratory MEMS *z*-axis rate gyroscope architecture that prioritizes the sense-mode quality factor and provides improved ordering of the mechanical vibrational modes. The proposed linearly coupled, dynamically balanced anti-phase sense-mode design minimizes substrate energy dissipation to maximize the quality factor. The levered drive-mode mechanism structurally forces the anti-phase drive-mode motion of the symmetrically decoupled tines eliminating the lower frequency spurious mode and providing true mechanical rejection of external shocks and accelerations. SOI prototypes were characterized in a vacuum chamber demonstrating drive-mode quality factor of 67,000 and ultra-high sense-mode quality factor of 125,000. A vacuum packaging technology was introduced and demonstrated a ceramic package-level sealed gyroscope with a quality factor on the order of 100,000. The high quality factor and mode ordering of the new design provide a path toward ultra-high scale factor without compromising the sensitivity to external accelerations.

© 2010 Elsevier B.V. All rights reserved.

1. Introduction

The operation of micromachined vibratory gyroscopes is based on a transfer of energy between two vibrational modes of a proof mass due to the Coriolis effect [1]. A very common class of Coriolis vibratory gyroscopes are implemented as tuning forks, consisting of two mechanically or electrically coupled proof masses (or equivalently, tines) operated in anti-phase. The advantage of the tuning fork architecture is its ability to reject common mode acceleration inputs by enabling a differential Coriolis measurement between the two tines [2,3]. Additionally, the anti-phase operation of the vibrational modes minimizes substrate energy dissipation allowing increasingly larger quality factors [4]. By matching the drive- and the sense-modes, the sensitivity and noise performance of the rate sensor can be increased proportional to the sense-mode quality factor [5].

Conventional silicon tuning fork architectures, however, present two major design drawbacks. First, the coupling of the proof masses introduces an in-phase structural mode at a frequency lower than the operational anti-phase mode. While a differential measurement of the Coriolis signal can help minimize the effect of the common mode proof mass motion, the scheme is prone to drifts due to nonlinear capacitive detection effects caused by large displacements [6]. Secondly, the mode designation can have a dramatic effect on the realized quality factors. When the linearly coupled resonant system is chosen as the drive, the maximal achievable sense-mode quality factor is limited to approximately half of the drive-mode [7,8] due to substrate energy dissipation caused by the coupled tine torque imbalance [9].

Recently, a new dual mass tuning fork gyroscope architecture was introduced [10], which addresses the limitations of the conventional designs. Unlike previous tuning fork implementations, the proposed architecture operates the linearly coupled, anti-phase resonant system as the sense-mode, which prioritizes the sense-mode quality factor by mechanical design. Since this mode is balanced in both linear momentum as well as moment of reaction forces (torque), the energy dissipation through the substrate is effectively eliminated; the increasingly large quality factors enabled by this mode designation provides a path toward ultra-high mechanical sensitivity to the input angular rate through mode-matching when operated in vacuum. To address the parasitic, lower frequency in-phase mode, the proposed design uses a levered coupling mechanism in the drive-mode as opposed to a conventional linear flexure. This provides the proposed design with true mechanical rejection of external shocks and accelerations by shifting the spurious in-phase mode above the operational anti-phase frequency.

In this paper, we present a more complete account of the new design, as well as experimental characterization of a second generation implementation with improved structural response characteristics and stand alone vacuum packaging. A detailed description of the design architecture is given in Section 2. Section 3 presents the experimental characterization of the structural and rate responses. Measurement of ultra-high quality factors and

* Corresponding author.
E-mail address: alex.trusov@gmail.com (A.A. Trusov).

0924-4247/$ – see front matter © 2010 Elsevier B.V. All rights reserved.
doi:10.1016/j.sna.2010.01.007

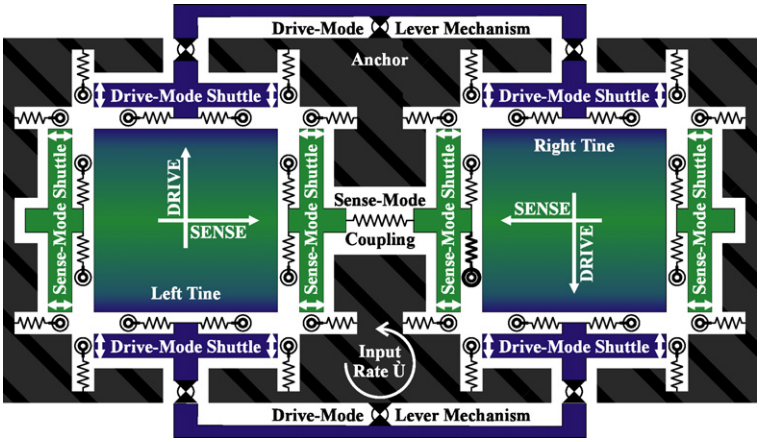

Fig. 1. Structural schematic of the proposed gyroscope architecture with levered anti-phase drive-mode and linearly coupled anti-phase sense-mode for maximization of sense-mode *Q*-factor.

analysis of the coupled design advantages are discussed in Section 4. Section 5 reports a second generation implementation with improved structural response and stand alone vacuum packaging. Scaling of gyroscope performance with increasing quality factor is analyzed in Section 6. Finally, Section 7 concludes the paper with a summary of obtained results.

2. Design concept

The proposed dual mass mechanical architecture, Fig. 1, comprises two identical tines, a lever mechanism for synchronization of the anti-phase drive-mode motion, and coupling flexures for the linear anti-phase sense-mode. Each symmetrically decoupled tine [11] consists of an anchored outer frame, two drive-mode and two sense-mode shuttles, and a proof mass. The drive-mode and sense-mode shuttles are suspended in the *x*–*y* plane relative to the substrate by pairs of springs. These flexures restrict the motion of the shuttles solely to their respective axes. Suspension elements of identical geometry couple the shuttles to their respective proof masses. Proof masses of both tines are suspended in the *x*–*y* plane with equal effective stiffnesses. The symmetry of the tines improves robustness of drive- and sense-mode frequency positioning (the two resonant frequencies are maintained equal in the mode-matched case) to fabrication imperfections and temperature induced shifts of resonant frequencies.

2.1. Drive-mode design

The drive-mode of the dual mass gyroscope is formed by the two tines forced into anti-parallel, anti-phase motion synchronized by the mechanical system that allows angular displacement of the coupling levers with respect to the anchored pivot, Fig. 2. Rigidity of the levering mechanism to the in-phase displacement eliminates any lower frequency mode of vibration and shifts

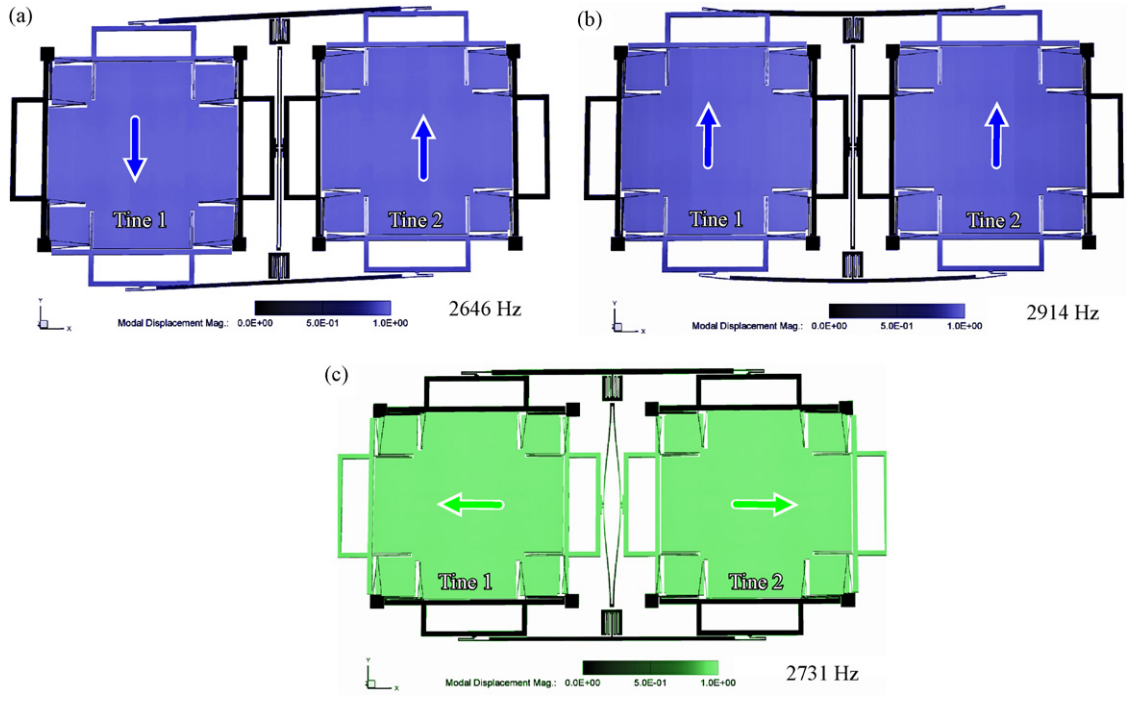

Fig. 2. Finite element modeling of the levered tuning fork gyroscope. The implementation utilizes symmetrically decoupled tines with a linear sense-mode coupling spring and a drive-mode levering mechanism. (a) Levered anti-phase drive-mode at 2646 Hz. (b) In-phase drive-mode resonance is shifted to a higher frequency of 2914 Hz. (c) Linearly coupled anti-phase sense-mode at 2731 Hz.

the in-phase drive-mode above the operational frequency of the device, Fig. 2. The intentional mode arrangement improves the phase stability [12] and enables true mechanical rejection of common mode accelerations and shocks.

2.2. Sense-mode design

While achieving high sense-mode quality factors is essential to improve sensitivity and precision of vibratory gyroscopes, the quality factors of vibrating microstructures in vacuum are often limited by the dissipation of energy through the substrate due to linear momentum and torque imbalances [9]. The sense-mode of the proposed gyroscope is formed by the two linearly coupled tines moving in anti-phase to each other in response to the anti-phase Coriolis input, Fig. 2. Unlike conventional tuning fork gyroscopes, the new architecture prioritizes the quality factor of the sense-mode by mechanical design, where the linearly coupled anti-phase sense-mode is balanced in both the linear momentum as well as torque in order to minimize the dissipation of energy through the substrate. Unlike the drive-mode direction, common mode rejection along the sense-mode of the current design is done electrically similarly to other MEMS tuning fork devices [13]. To provide the linear anti-phase sense-mode with mechanical rejection of common mode accelerations a coupling flexure based on semi-circular [12] or levered [10] structures can used in the future implementations.

2.3. Actuation and detection

The gyroscope is electrostatically driven into anti-phase motion using driving voltages imposed across the differential lateral comb electrodes on the drive-mode shuttles. During rotation around the *z*-axis, the Coriolis acceleration of the proof masses induces linear anti-phase sense-mode vibrations which are capacitively detected using differential parallel plate electrodes on the sense-mode shuttles.

3. Structural and rate characterization

In this section, we report experimental characterization of micromachined prototypes of the proposed dual mass gyroscope architecture.

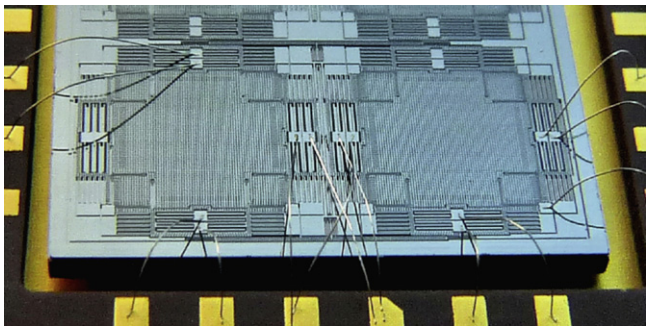

Fig. 3. Optical photograph of a packaged tuning fork gyroscope.

3.1. Prototype fabrication

The fabrication of prototypes was done using an in-house, wafer-level, single-mask process using silicon-on-insulator (SOI) wafers with a 50-μm thick device layer and a 5 μm buried oxide layer. After patterning photoresist with the device mask, the wafers were subjected to Deep Reactive Ion Etching (DRIE) using a Surface Technology Systems (STS) Advanced Silicon Etching (ASE) tool. The minimal feature of 5 μm was used to define capacitive gaps. The perforated structures were released using a timed 20% HF acid bath. For convenient characterization, individual devices were packaged using 24 pin ceramic, dual-in-line (DIP) packages and wirebonded as illustrated in Fig. 3.

3.2. Structural characterization

Structural characterization of a prototype operated in air is shown in Fig. 4. As predicted by the modeling in Fig. 2, the anti-phase levered operational mode at 2483 Hz is the lowest frequency mode along the drive direction, while all the spurious modes are shifted to higher frequencies. For the tested prototype, the in-phase drive-mode is at 2781 Hz, which can be increased even farther by stiffening the U-shaped flexures located at the tips of the drive-mode synchronization levers.

The untrimmed anti-phase sense-mode resonance was measured at 2538 Hz, which is 55 Hz above the drive-mode operational frequency. The device can be operated in air without frequency tuning providing a practically feasible bandwidth on the order

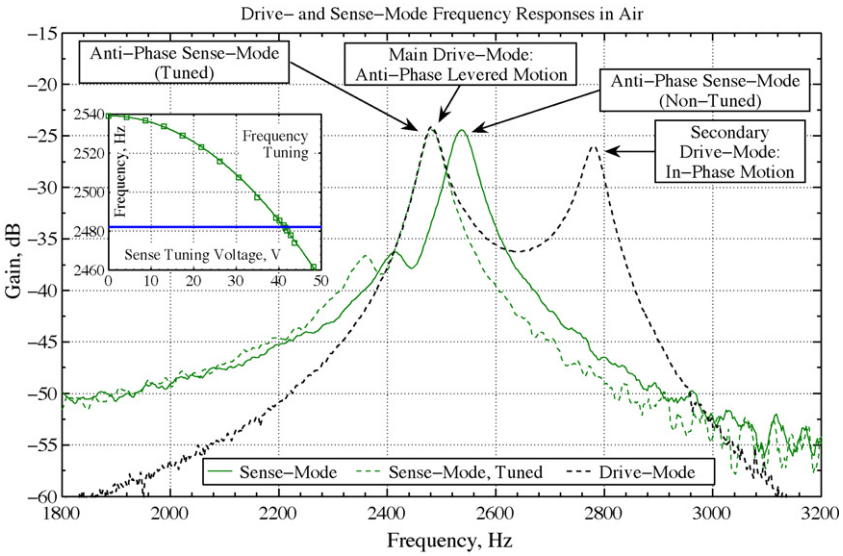

Fig. 4. Measured frequency responses of the drive- and the sense-modes in air. Inset: Electrostatic tuning of frequency for mode-matching.

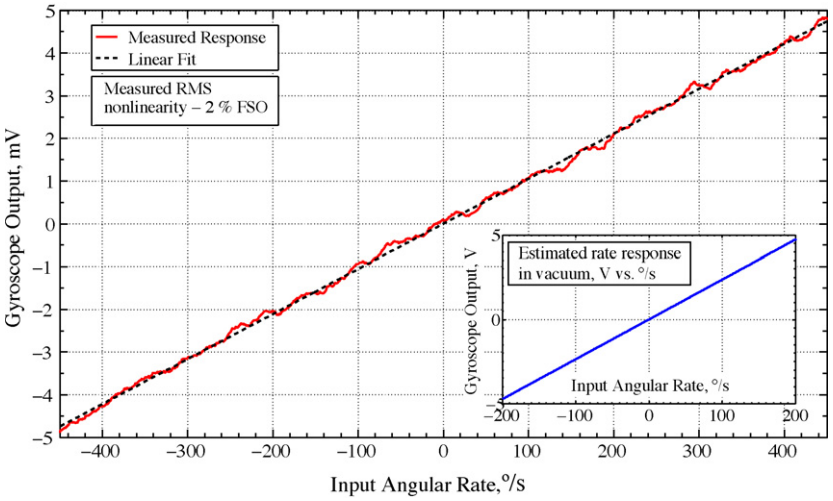

Fig. 5. Measured rate response in air (sense-mode quality factor 65, RMS nonlinearity 2% FSO). Sensitivity improves more than 2000 times in vacuum.

of 50 Hz. For ultra-high sensitivity, mode-matched operation at reduced pressures, the sense-mode resonance can be tuned down to 2483 Hz using the electrostatic negative spring effect as shown in the inset of Fig. 4.

3.3. Rate characterization

The angular rate performance of the prototype was experimentally characterized in air using a computer-controlled Ideal Aerosmith 1291BR rate table. The gyroscope was driven into the anti-phase resonant motion with a 5 μm amplitude using a combination of a 30 V DC bias and a 3.5 V_{RMS} AC driving voltage applied to the anchored differential drive-mode lateral-comb electrodes. A differential electromechanical amplitude modulation (EAM) technique [6] was used to detect the Coriolis-induced motion in the sense-mode. The AC carrier voltage with 3.5 V_{RMS} amplitude at 80 kHz frequency was applied to the mobile masses. The anchored differential sense-mode parallel-plate electrodes were connected to the inputs of a two-stage differential transimpedance amplification circuit. An experimentally measured rate response of the prototype in atmospheric pressure is shown in Fig. 5, confirming Coriolis functionality of the proposed mechanical sensor element architecture.

4. Ultra-high quality factor operation

In this section, we report experimental results on ultra-high quality factor operation and analysis of the coupled design advantages.

4.1. Experimental characterization of quality factors

The limiting non-viscous quality factors of the drive- and sense-modes were characterized using a custom vacuum chamber pumped to approximately 0.1 mTorr in order to eliminate effects of gas damping. As shown in Fig. 6, the measured quality factor of the drive-mode in vacuum increases to 67,000, which allows driving the gyroscope with just 3 mV_{RMS} AC driving voltage combined with a 30 V DC polarization voltage. While the anti-parallel, anti-phase drive-mode is balanced in linear momentum, the quality factor is limited by the dissipation of energy through the substrate due to the non-zero torque. In contrast, as shown in Fig. 7, the measured limiting quality factor of the sense-mode reaches 125,000 due to the optimized mechanical design with minimized energy dissipation.

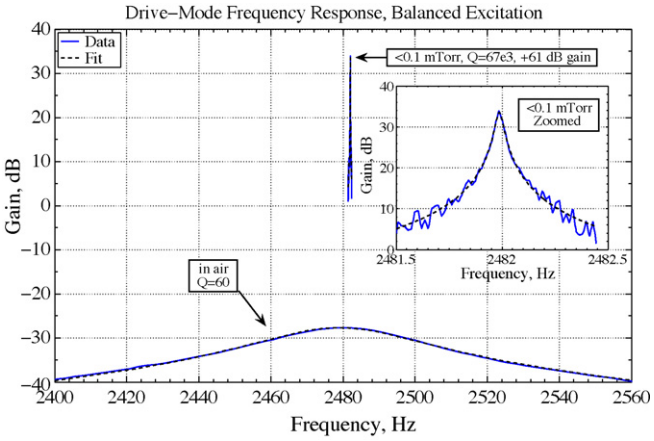

Fig. 6. Measured frequency response of the levered anti-phase drive-mode in air ($Q = 60$), and in vacuum ($Q = 67{,}000$).

4.2. Comparison to single-mass gyroscope

A single-mass gyroscope identical to one uncoupled tine was also fabricated and characterized to analyze the advantages of the proposed tuning fork architecture. For the single-mass device, the limiting non-viscous quality factor of both the drive- and the

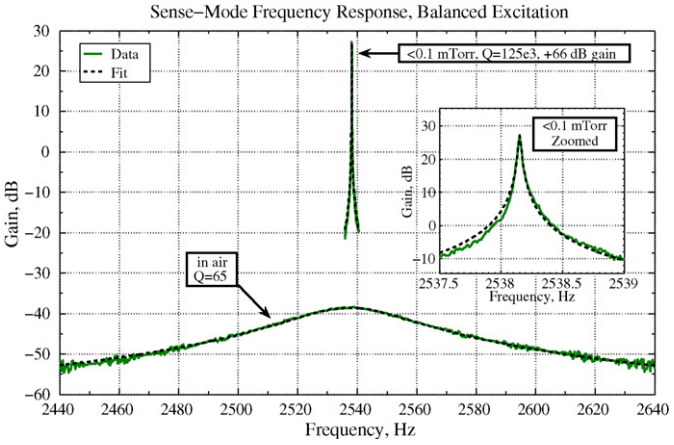

Fig. 7. Measured frequency response of the momentum and torque balanced linear anti-phase sense-mode in air ($Q = 65$), and in vacuum ($Q = 125{,}000$).

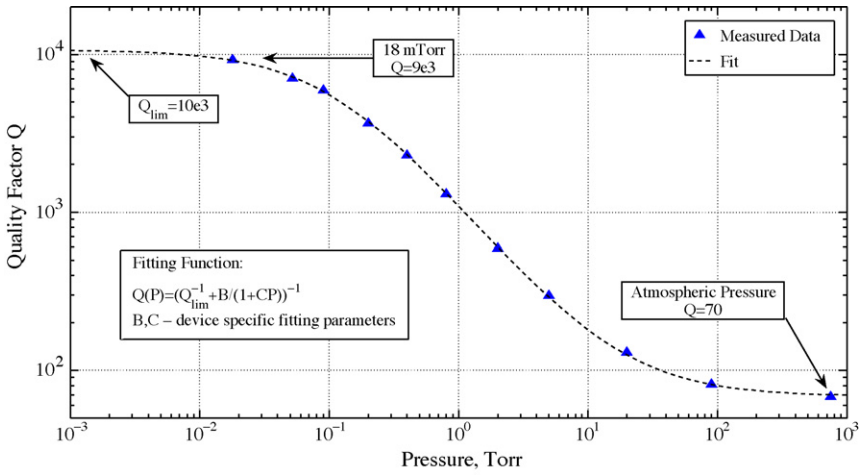

Fig. 8. Measured quality factor versus pressure for an individual, uncoupled tine. The quality factor is limited by the energy dissipation through the substrate.

sense-modes is 10,000, as shown in Fig. 8. Momentum balance of the tuning fork drive-mode results in a 6.7 times improvement of the quality factor; momentum and torque balance of the tuning fork sense-mode allows a 12.5 times improvement in quality factor and sensitivity.

The experimental comparison of the proposed dual mass tuning fork gyroscope to a single-mass device confirms the design hypotheses. Linear momentum balance improves the quality factor of a vibratory mode by 5–10 times; complete linear momentum and torque balance improves the quality factor by more than 10 times.

5. Second generation implementation

In this section, we present a second generation implementation with improved structural response, and introduce a vacuum packaging approach for stand alone high-Q gyroscopes.

5.1. Improved structural characteristics

While the previously described first generation prototype experimentally confirmed the design hypotheses on sense-mode quality factor optimization and mode ordering, several adjustments to the physical layout are desired. First, the main anti-phase drive-mode frequency should be slightly above the anti-phase sense-mode to reduce the nominal frequency mismatch and allow the electrostatic tuning of the drive-mode instead of the sense-mode (tuning of the sense-mode using an electrostatic negative spring enables coupling of the DC voltage noise into the detection channel). At the same time, the separation between the main anti-phase drive-mode and the higher frequency parasitic in-phase mode should be increased to further improve the mechanical rejection of common mode acceleration inputs.

Based on the experimental results and several iterations of finite element analysis, a second generation prototype of the gyroscope architecture was designed to address the outlined improvements, Fig. 9. Two springs were added to the main pivots of the drive-mode synchronization mechanisms to slightly increase the drive-mode frequency and suppress the parasitic lever translational modes. The levers were also redesigned for higher bending stiffness to further suppress the in-phase mode along the drive direction.

The new prototypes were fabricated using the previously described SOI process and experimentally characterized. Frequency responses of the drive- and sense-modes measured in air are shown in Fig. 10. The separation between the main anti-phase drive-mode and the higher frequency parasitic in-phase mode is improved five times from 11% (2483 and 2781 Hz, respectively) to 58% (1698 and 2680 Hz, respectively). Unlike the first implementation, the drive-mode has a higher frequency than the sense-mode, with a twice smaller nominal separation than the first generation implementation (from 55 to 23 Hz).

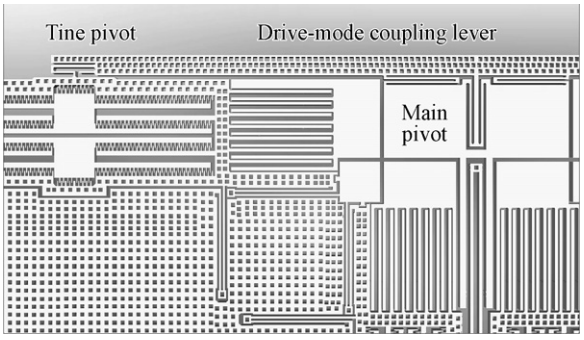

Fig. 9. Solid model of a second generation drive-mode lever mechanism. Additional springs in the main pivots suppress the parasitic modes of lever motion.

5.2. Vacuum packaging

A package-level technology for the robust sealing of the high-Q gyroscopes in sub-mTorr cavity pressures was developed to allow experimental characterization of stand alone sensors, Fig. 11. The packaging procedure comprises the attachment of a gyroscope die

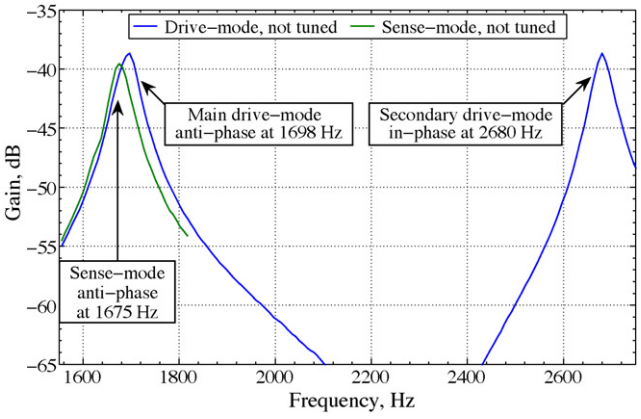

Fig. 10. Measured frequency responses of the second generation drive- and the sense-modes in air, showing the improved mode ordering.

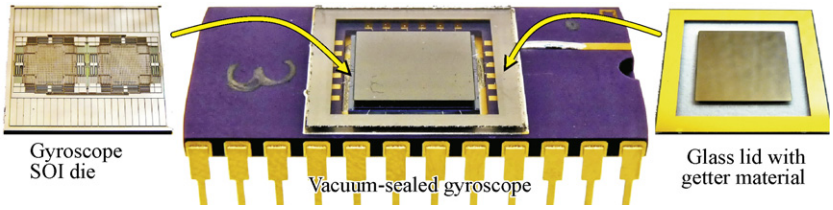

Fig. 11. Optical photograph of a vacuum packaged tuning fork gyroscope, showing the die, the ceramic package, and the glass lid with getter material and metal sealing ring.

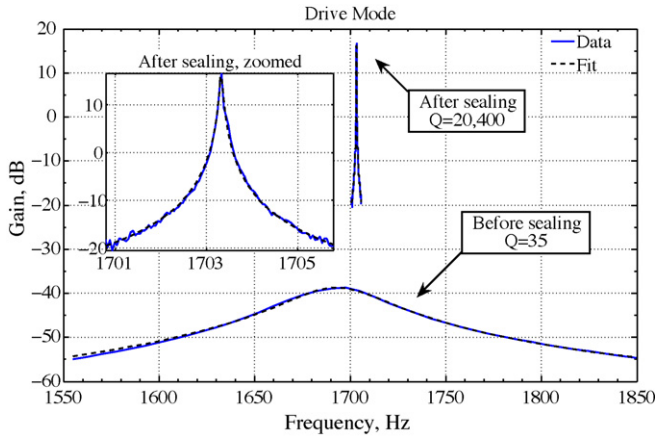

Fig. 12. Measured frequency response of the levered anti-phase drive-mode in air ($Q = 35$), and after the vacuum packaging ($Q = 20{,}400$).

to a ceramic package followed by the vacuum sealing of the device within the cavity. Both the die and lid attachment rely on fluxless gold–tin eutectic solder bonding of metalized surfaces in order to minimize outgassing of the bond material and to eliminate corrosion of the sealed device by flux residue. The rigid eutectic bonding of the die and package is desired for minimization of energy dissipation in the anti-phase devices with fabrication imperfections [9]. To provide a sustainable vacuum inside the package cavity, a getter material deposited by SAES Getters on the lids was activated in 10^{-6} Torr vacuum, followed by the lid sealing.

The second generation prototypes of the proposed tuning fork gyroscope were packaged using the described procedure. A complete vacuum packaged gyroscope, Fig. 11, was experimentally characterized to determine the ultimate sealed cavity pressure. Figs. 12 and 13 present measured frequency responses of the drive- and sense-modes, respectively, before and after vacuum sealing. The combination of the anti-phase design and packaging process resulted in stand-alone quality factors of 20,000 and 91,000, respectively. Normalization of the measured ultra-high sense-mode quality factor to the resonant frequency indicates sub-mTorr vacuum level in the sealed package. In order to investigate the long term stability of the vacuum package, frequency response of the anti-phase sense-mode was measured again four months later, Fig. 14. The measured quality factor of 93,456 was within 2% of the original value, indicating long term robustness of the vacuum packaging technology. It should be noted that the effective frequency resolution (spacing between frequency sweep datapoints) of the used experiment setup was approximately 10 mHz. This is on the same order as the 3-dB bandwidth of a 1.7 kHz device with a quality factor of 100,000. The 2% discrepancy between the two quality factor measurements is attributed to this inherent limitation of the frequency sweep approach. Ring-down tests are expected to yield more accurate quality factor measurements for such high-Q devices.

6. Effects of quality factor on performance

In this section, we analyze the effects of quality factor scaling on performance of vibratory gyroscopes.

6.1. Scaling of mechanical sensitivity

Improvement of the gyroscope scale factor is one of the main advantages of increasing the sense-mode quality factor. By evaluating the single-DOF sense-mode transfer function at the operational frequency and substituting Coriolis acceleration as the input to the system, the following expression is obtained:

$$SF = 9.7e3\frac{QA}{\omega_y}\ \mathrm{nm/(^\circ/h)},$$

where Q is the sense-mode quality factor, A the amplitude of the drive-mode motion in μm, ω_y the mode-matched operational frequency in rad/s, and SF is the amplitude of the sense-mode vibrations in nm for the rate input of $1^\circ\,\mathrm{h}^{-1}$. The scale factor equation

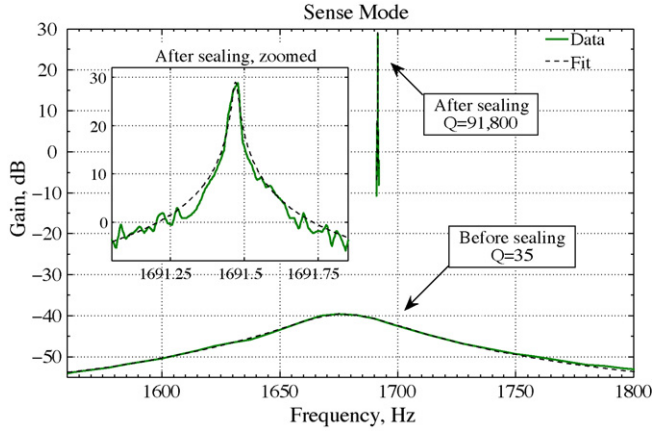

Fig. 13. Measured frequency response of the anti-phase sense-mode in air ($Q = 35$), and after the vacuum packaging ($Q = 91,800$).

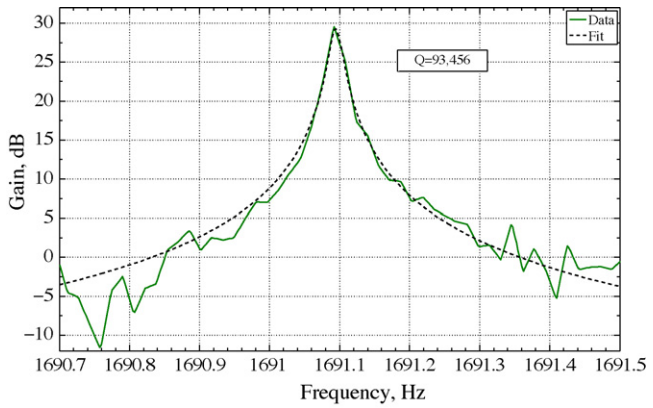

Fig. 14. Frequency response of the anti-phase sense-mode measured four months after the vacuum sealing. The measured Q of 93,456 is within 2% of the original value, which demonstrates long term robustness of the vacuum packaging technology.

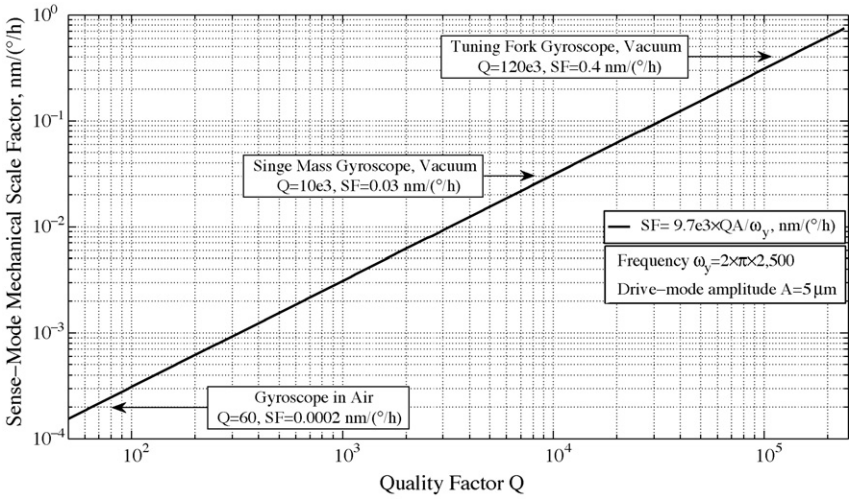

Fig. 15. Effects of sense-mode quality factor on the mechanical scale factor of a mode-matched gyroscope.

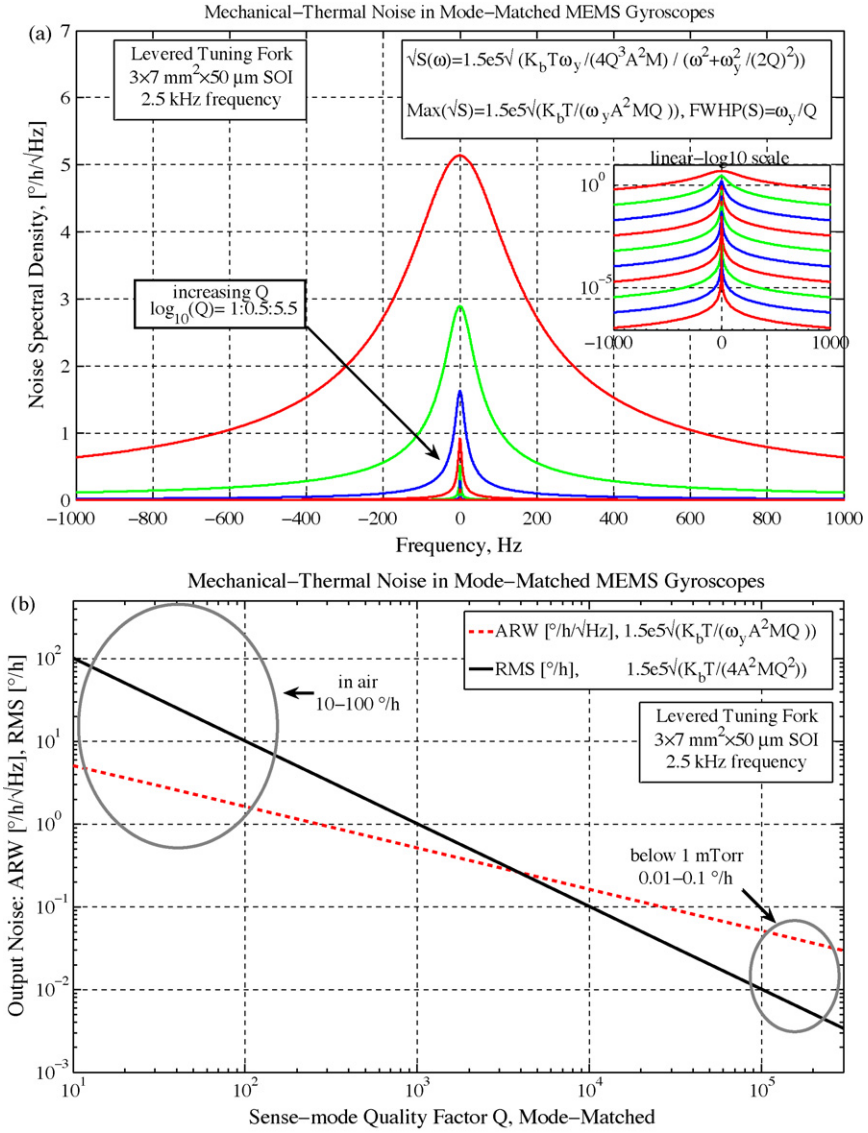

Fig. 16. Effects of sense-mode quality factor on mechanical–thermal noise (MTN) of a mode-matched gyroscope. (a) Scaling of the MTN spectral density with increasing quality factor. (b) Scaling of the MTN root-mean-square (RMS) and Angle Random Walk (ARW) with increasing quality factor.

shows that maximization of the mechanical sensitivity requires prioritization of the sense-mode quality factor, large amplitude of drive-mode motion, and low operational frequency. The design proposed in this paper meets these three criteria without compromising robustness to external accelerations by using a lumped, decoupled, anti-phase structures.

Effect of the sense-mode quality factor on the mechanical scale factor of the proposed tuning fork gyroscope is shown in Fig. 15. The ultra-high quality factor of the proposed gyroscope translates into mechanical sensitivity of 0.4 nm/(°/h) when operated mode-matched in vacuum. For state-of-the-art integrated electronics, it is not unprecedented to detect sub-angstrom displacements of the sense-mode. For instance, detectable movement of 16 Fermi (or, equivalently, 16×10^{-15} m, or 0.00016 Å) is reported in [14]. The proposed tuning fork gyroscope architecture provides a path to minimizing the effect of the detection electronics noise by utilizing ultra-high mechanical scale factor of the sense-mode.

6.2. Scaling of mechanical–thermal noise

As shown in the previous section, higher mechanical sensitivity reduces the effect of the electronics noise when measured in the units of the angle rate. It is thus important to analyze the fundamental noise performance limits imposed by the mechanical–thermal noise [15] in the structure of the gyroscope. Fig. 16 shows scaling of the mechanical–thermal noise performance of the gyroscope computed based on the analytical model derived in [16,17]. The fundamental mechanical–thermal noise performance limit improves from $\approx 10^{\circ}\,h^{-1}$ RMS in air to $0.01^{\circ}\,h^{-1}$ RMS in vacuum. The mechanical–thermal noise performance of the gyroscope can be improved further by increasing the mass of the structure (for instance, by increasing the thickness from the current 50 μm), lowering the operational frequency, and further increasing the sense-mode quality factor (for instance, by tightening the fabrication tolerances to improve the symmetry of the fabricated structures [9]).

7. Conclusions

This paper proposed and demonstrated a new tuning fork gyroscope design architecture, which utilizes symmetrically decoupled tines with drive-mode synchronization and sense-mode coupling structures. The levered drive-mode mechanism structurally forces the anti-parallel, anti-phase drive-mode motion and eliminates the lower frequency spurious mode present in conventional tuning fork gyroscopes. The linearly coupled, momentum and torque balanced anti-phase sense-mode reduces dissipation of energy through the substrate yielding ultra high quality factors. Prototypes characterized in a vacuum chamber demonstrated drive-mode quality factor of 67,000 and sense-mode quality factor of 125,000, enabling an ultra-high mechanical scale factor of 0.4 nm of sense-mode displacement per $1^{\circ}\,h^{-1}$ of input angular rate. A vacuum packaging technology was introduced and demonstrated a ceramic package-level sealed gyroscope with a quality factor on the order of 100,000.

The high quality factor and mode ordering of the new design provide a path to ultra-high rate sensitivity without compromising the susceptibility to external accelerations. The new tuning fork gyroscope architecture is especially suitable for applications such as gyrocompassing, where ultra-high precision inertial measurements are required in a relatively low bandwidth.

Acknowledgements

This work was supported by the Office of Naval Research/Naval Surface Warfare Center contract N00178-08-C1014. The authors would like to acknowledge University of California, Irvine Integrated Nanosystems Research Facility (INRF) for assistance with the fabrication of prototypes, David Virissimo of Semiconductor Packaging Materials for advice on die attachment, Heather Florence of SAES Getters and Paul Barnes of SST International for assistance with vacuum packaging of prototypes. The gyroscopes were designed and characterized at the MicroSystems Laboratory, University of California, Irvine.

References

[1] A.M. Shkel, Type I and type II micromachined vibratory gyroscopes, in: Proc. IEEE/ION Position, Location, and Navigation Symposium, 2006, pp. 586–593.
[2] M.S. Weinberg, A. Kourepenis, Error sources in in-plane silicon tuning-fork MEMS gyroscopes, J. Microelectromech. Syst. 15 (3) (2006) 479–491 (doi:10.1109/JMEMS.2006.876779).
[3] U.-M. Gomez, B. Kuhlmann, J. Classen, W. Bauer, C. Lang, M. Veith, E. Esch, J. Frey, F. Grabmaier, K. Offterdinger, T. Raab, H.-J. Faisst, R. Willig, R. Neul, New surface micromachined angular rate sensor for vehicle stabilizing systems in automotive applications, in: Proc. International Solid-State Sensors, Actuators and Microsystems Conference TRANSDUCERS 2005, vol. 1, 2005, pp. 184–187 (doi:10.1109/SENSOR.2005.1496389).
[4] A.A. Trusov, A.R. Schofield, A.M. Shkel, Study of substrate energy dissipation mechanism in in-phase and anti-phase micromachined vibratory gyroscopes, in: Proc. IEEE Sensors, 2008, pp. 168–171 (doi:10.1109/ICSENS.2008.4716410).
[5] N. Yazdi, F. Ayazi, K. Najafi, Micromachined inertial sensors, Proc. IEEE 86 (8) (1998) 1640–1659, doi:10.1109/5.704269.
[6] A.A. Trusov, A.M. Shkel, Capacitive detection in resonant MEMS with arbitrary amplitude of motion, J. Micromech. Microeng. 17 (8) (2007) 1583–1592.
[7] M.F. Zaman, A. Sharma, F. Ayazi, High performance matched-mode tuning fork gyroscope, in: Proc. MEMS 2006 Istanbul Micro Electro Mechanical Systems 19th IEEE International Conference, 2006, pp. 66–69 (doi:10.1109/MEMSYS.2006.1627737).
[8] M.F. Zaman, A. Sharma, Z. Hao, F. Ayazi, A mode-matched silicon-yaw tuning-fork gyroscope with subdegree-per-hour Allan deviation bias instability, J. Microelectromech. Syst. 17 (6) (2008) 1526–1536, doi:10.1109/JMEMS.2008.2004794.
[9] A.A. Trusov, A.R. Schofield, A.M. Shkel, A substrate energy dissipation mechanism in in-phase and anti-phase micromachined *z*-axis vibratory gyroscopes, J. Micromech. Microeng. 18 (9) (2008) 095016 (10 pp., http://stacks.iop.org/0960-1317/18/095016).
[10] A.A. Trusov, A.R. Schofield, A.M. Shkel, Gyroscope architecture with structurally forced anti-phase drive-mode and linearly coupled anti-phase sense-mode, in: Proc. International Solid-State Sensors, Actuators and Microsystems Conference TRANSDUCERS, Denver, Colorado, USA, 2009.
[11] M.S. Kranz, G.K. Fedder, Micromechanical vibratory rate gyroscope fabricated in conventional CMOS, in: Symposium Gyro Technology, Stuttgart, Germany, 3.0-3, 1997, p. 8.
[12] K. Azgin, Y. Temiz, T. Akin, An SOI-MEMS tuning fork gyroscope with linearly coupled drive mechanism, in: Proc. MEMS Micro Electro Mechanical Systems IEEE 20th International Conference, 2007, pp. 607–610 (doi:10.1109/MEMSYS.2007.4433080).
[13] A.R. Schofield, A.A. Trusov, A.M. Shkel, Multi-degree of freedom tuning fork gyroscope demonstrating shock rejection, in: Proc. IEEE Sensors Conference, 2007, pp. 120–123 (doi:10.1109/ICSENS.2007.4388350).
[14] J.A. Geen, S.J. Sherman, J.F. Chang, S.R. Lewis, Single-chip surface micromachined integrated gyroscope with $50^{\circ}\,h^{-1}$ Allan deviation, IEEE J. Solid-State Circuits 37 (12) (2002) 1860–1866, doi:10.1109/JSSC.2002.804345.
[15] T. Gabrielson, Mechanical–thermal noise in micromachined acoustic and vibration sensors, IEEE Trans. Electron Dev. 40 (5) (1993) 903–909, doi:10.1109/16.210197.
[16] R. Leland, Mechanical–thermal noise in vibrational gyroscopes, in: Proc. American Control Conference, vol. 4, 2001, pp. 3256–3261 (doi:10.1109/ACC.2001.946424).
[17] R. Leland, Mechanical–thermal noise in MEMS gyroscopes, IEEE Sens. J. 5 (3) (2005) 493–500, doi:10.1109/JSEN.2005.844538.

Biographies

Alexander A. Trusov received the diploma in applied mathematics and mechanics from the Moscow State University, Moscow, Russia in 2004 and the MS and PhD degrees in mechanical and aerospace engineering from the University of California, Irvine in 2006 and 2009, respectively. He is currently a project scientist at the UC Irvine MicroSystems laboratory where he is leading several federal funded programs on high performance inertial microsystems. His research interests include design, modeling, fabrication, and vacuum packaging of micromachined inertial systems, design of characterization experiments, and statistical data processing and analysis. He has published over 20 journal and international conference papers on MEMS inertial sensors and serves as a reviewer for major journals in the fields of MEMS and sensors. He is a member of the American Society of Mechanical Engineers (ASME), and the Institute of the Institute of Electrical and Electronics Engineers (IEEE).

Adam R. Schofield received the BS degree summa cum laude with honors and the MS degree (supported by an Ohio Space Grant Fellowship) in mechanical engineering from the University of Dayton, in 2002 and 2005, respectively. In 2009, he received the PhD degree in mechanical and aerospace engineering from the University of California, Irvine where his research focused on the design, fabrication, packaging, and characterization of MEMS inertial sensors. He has recently joined System Planning Corporation (SPC) in Arlington, VA, as a senior scientist where he provides technical support to the Microsystems Technology Office (MTO) of the Defense Advanced Research Projects Agency (DARPA). His current technical interests are the design and packaging of high-performance micromachined inertial sensors for navigation and positioning, microsystems for thermal management, and energy harvesting and micro power storage MEMS for ultra-portable, energy efficient systems. He was awarded the Class of 2002 Award for Outstanding Mechanical Engineering Achievement by the University of Dayton and is a member of the Institute of Electrical and Electronics Engineers (IEEE), the American Society of Mechanical Engineers (ASME), as well as the Tau Beta Pi, Pi Tau Sigma, and Golden Key Honor Societies.

Andrei M. Shkel received the diploma degree (with excellence) in mechanics and mathematics from Moscow State University, Moscow, Russia, in 1991, and the PhD degree in mechanical engineering from the University of Wisconsin, Madison, in 1997. He is a Program Manager in the Microsystems Technology Office of the Defense Advanced Research Projects Agency (DARPA), Arlington, VA; he is serving in this capacity while on leave from his faculty position as a professor in the Department of Mechanical and Aerospace Engineering at University of California, Irvine, CA, where he is also the Director of the UCI Microsystems Laboratory. He is the holder of twelve U.S. and international patents. His professional interests are reflected in more than 100 publications. He is an editor of the IEEE JMEMS. He is the recipient of the 2006 UCI Research Award, the 2005 NSF CAREER Award, and the 2002 George E. Brown, Jr., Award.